The American Journal of Pathology, Vol. 175, No. 4, October 2009

DOI: 10.2353/ajpath.2009.090007

Tumorigenesis and Neoplastic Progression

Modulation of the Tumor Suppressor Protein α-Catenin by Ischemic Microenvironment

Claire L. Plumb, Una Adamcic, Siranoush Shahrzad, Kanwal Minhas, Sirin A.I. Adham, and Brenda L. Coomber

From the Department of Biomedical Sciences, Ontario Veterinary College, University of Guelph, Guelph, Canada

Dysregulation or mislocalization of cell adhesion molecules and their regulators, such as E-cadherin, β-catenin, and α-catenin, usually correlates with loss of polarity, dedifferentiation, invasive tumor growth, and metastasis. A subpopulation of α-catenin-negative cells within the DLD-1 colorectal carcinoma cell line causes it to display a heterogeneous morphological makeup, thus providing an excellent model system in which to investigate the role of α-catenin in tumorigenesis. We re-established expression of α-catenin protein in an α-catenin-deficient subpopulation of the DLD-1 cell line and used it to demonstrate that loss of α-catenin resulted in increased *in vitro* tumorigenic characteristics (increased soft agarose colony formation, clonogenic survival after suspension, and survival in suspension). When the cells were used to form tumor xenografts, those lacking α-catenin showed faster growth rates because of increased cellular cycling but not increased tumor microvascular recruitment. α-Catenin-expressing cells were preferentially located in well perfused areas of xenografts when tumors were formed from mixed α-catenin-positive and -negative cells. We therefore evaluated the role of the ischemic tumor microenvironment on α-catenin expression and demonstrated that cells lose expression of α-catenin after prolonged exposure *in vitro* to hypoglycemic conditions. Our findings illustrate that the tumor microenvironment is a potent modulator of tumor suppressor expression, which has implications for localized nutrient deficiency and ischemia-induced cancer progression. ***(Am J Pathol 2009, 175:1662–1674; DOI: 10.2353/ajpath.2009.090007)***

The ability of carcinomas to invade and to metastasize depends largely on the degree of epithelial differentiation within the tumors.[1,2] The frequent loss of cell adhesion in epithelial cancers suggests that loss of E-cadherin expression or function may be partly responsible for the transition from adenoma to carcinoma, thus mediating local invasion.[3] Dysregulation or mislocalization of cell adhesion molecules and their regulators, such as E-cadherin, β-catenin, and α-catenin, usually correlates with loss of polarity, dedifferentiation, invasive tumor growth, and metastasis.[4] During development, in a process termed epithelial-mesenchymal transition, epithelial cells acquire fibroblast-like properties and show reduced intercellular adhesion and increased motility.[5,6] The epithelial-mesenchymal transition program converges on two central features, E-cadherin down-regulation and cytoskeletal reorganization, and overlaps with cell processes that control cell adhesion, motility, invasion, survival, and differentiation.[6] These features are important in carcinogenesis; E-cadherin acts to sequester β-catenin at the plasma membrane and abrogate β-catenin signaling, and adhesion molecules maintain cell-cell anchorage and inhibit cellular morphology via their associated junctions.

Human epithelial α-catenin is a cytoplasmic 102-kDa protein encoded by the *CTNNA1* gene located on chromosome 5q31[7] with a pseudogene located on chromosome 5q21–22.[8,9] The gene encodes 906 amino acids and consists of 16 coding exons and at least 1 5-prime noncoding exon,[7] and the protein exists as either a monomer or a homodimer, each with different binding properties.[10,11] α-Catenin directs epithelial sheet formation via a mechanism in which formin-1 interacts with α-catenin, localizes to adherens junctions, and nucleates unbranched actin filaments, causing linear actin cable assembly at nascent adherens junctions.[12] Disruption of the α-catenin-formin-1 interaction blocks the assembly of radial actin cables and perturbs intercellular adhesion.[12] Monomeric α-catenin binds more strongly to E-cadherin/

Supported by the Canadian Cancer Society Research Institute (grant 016117 to B.L.C.); C.L.P. was a recipient of scholarship funding from the Natural Sciences and Engineering Research Council of Canada and the Ontario Graduate Scholarship Program.

Accepted for publication June 22, 2009.

Address reprint requests to B.L. Coomber, Ph.D., Department of Biomedical Sciences, OVC, University of Guelph, Guelph, ON, Canada, N1G 2W1. E-mail: bcoomber@uoguelph.ca.

β-catenin complexes, whereas dimeric α-catenin binds more readily to actin cytoskeleton filaments. α-Catenin suppresses Arp2/3-mediated actin polymerization (probably by competitive binding) and thus directly regulates actin filament organization.[10] Stabilized cell-cell interactions require direct attachment of α-catenin to F-actin to promote cadherin-mediated contact formation.[13]

A combination of intact E-cadherin, β-catenin, and α-catenin provides favorable prognostic value for patients with endometrial carcinoma, whereas a lack of any of these proteins is correlated with a poorer prognosis.[14] Mutations in β-catenin, E-cadherin, and α-catenin genes have been found in some human cancers, and reduced levels of E-cadherin and α-catenin are often prognostic markers for poor clinical outcome in squamous cell carcinoma.[15,16] Sequestering of β-catenin at the adherens junction by protein tyrosine phosphatase PCP-2 causes stabilization of adherens junctions by dephosphorylation of β-catenin, thus inhibiting β-catenin-mediated nuclear signaling.[17] Reductions in E-cadherin and α-catenin are thought to act by liberating β-catenin, freeing it to trigger TCF/LEF-mediated transcription and cause uncontrolled tumor growth.[18,19] However, after conditional ablation of α-catenin in murine skin the epidermis loses polarity and becomes hyperproliferative, yielding large masses that resemble squamous cell carcinoma *in situ*[20]. In contrast, activating mutations in β-catenin typically result in benign hair tumors (pilomatricomas) rather than epidermal squamous cell carcinoma.[21,22] Such findings are not consistent with a model of α-catenin acting as a tumor suppressor solely through sequestration of β-catenin.

Re-expression of α-catenin in ovarian carcinoma caused complete negation of soft agarose colony and xenograft formation.[23] The human lung cancer cell line PC9 expresses E-cadherin but only a small quantity of abnormally sized α-catenin. On transfection to express wild-type α-catenin, these cells regain cell-cell adhesion.[24,25] The presence of α-catenin also results in re-establishment of functional adherens junctions in lung epithelium, which reduces invasiveness and permits formation of compact spheroids when cells were plated above nonadherent substrates.[26–28] Phosphorylated α-catenin functions by maintaining epithelial positioning and polarity as well as by inhibiting cell transformation in NIH-3T3 cells.[29] Together these findings illustrate that α-catenin protein is required for cell-cell adhesion and tumor suppression.

The DLD-1 colorectal carcinoma cell line displays heterogeneous morphological makeup because of a subpopulation of α-catenin-negative cells.[30,31] Under the microscope these α-catenin-negative cells seem rounded, and cells lacking α-catenin are interspersed with contact-inhibited epithelial cells expressing the protein. Thus, the DLD-1 cell line provides an excellent model system in which to investigate the role of α-catenin in tumorigenesis. Derived from an adenocarcinoma of sporadic origin,[32] DLD-1 cells consistently grow as epithelial monolayers and show heterogeneity by producing discrete areas of rounding cells.[33] The α-catenin-negative status of the rounding subpopulation was not reversed with repeated passages *in vitro*[31]. In addition, the DLD-1 cell line genotype includes a dominant-negative mutation in *P53*,[34] truncating mutations of the DNA mismatch repair enzyme *MSH6*[35] and tumor suppressor *APC*,[36] and an activating mutation of one *KRAS* gene.[37]

Recently our laboratory determined that mismatch repair-deficient colorectal carcinoma cells could develop activating point mutations in the *KRAS* gene when exposed to ischemic conditions.[38,39] Here we evaluate the role of the ischemic tumor microenvironment on α-catenin expression in the context of mismatch repair deficiency. We found that cells in an ischemic microenvironment are prone to development of *CTNNA1* mutations leading to loss of α-catenin expression and that this loss leads to increased tumorigenicity *in vitro* and *in vivo*. Re-expression of exogenous α-catenin in null cells restored their less aggressive phenotype. This work supports the concept that features of the ischemic microenvironment in solid tumors (and by extension, agents that modulate it) can influence tumor suppressor expression, leading to increased tumor aggressiveness and progression of disease.

Materials and Methods

Cells and Culture Conditions

All materials and supplies were obtained from Fisher Scientific (Mississauga, ON) unless otherwise noted. DLD-1 cells (American Type Culture Collection, Manassas, VA) and their subclones were maintained in Dulbecco's modified Eagle's medium (DMEM) (Sigma-Aldrich, St. Louis, MO) supplemented with 10% fetal bovine serum, 50 μg/ml gentamicin, 1 mmol/L sodium pyruvate, and 5 μl/ml Fungizone antimycotic (all Sigma-Aldrich) at 37°C in a humidified atmosphere containing 5% CO_2. To obtain pure populations of the DLD-1 cell line with rounding or epithelial morphologies, the DLD-1 parent cell line was serially diluted in culture medium and plated in 96-well culture plates; the presence of a single cell/well was visually verified using a phase-contrast microscope. Cells were maintained under standard culture conditions and allowed to establish colonies. Multiple colonies were subcloned by a second round of serial dilution followed by clonal expansion, resulting in clones having either the epithelial or rounding morphologies. One clone from each of the epithelial and rounding subtypes was used for the ensuing studies; these two clones were termed as PC7 (epithelial) and L2a (rounded). PC7 clone cells expressed α-catenin in culture and maintained α-catenin expression when used to produce xenografts in immune-deficient mice. L2a clone cells lacked detectable α-catenin. The α-catenin status was used as a marker for the clonal population in experiments in which the two populations were mixed. Both PC7 and L2a cell lines were used within 10 passages of the inception of these studies to minimize genetic drift in these clones.

For monolayer growth rates, 1×10^5 cells were plated in triplicate and counted by hemocytometer daily for a period of 5 days. The influence of the glucose-deficient environment was determined when α-catenin-expressing

PC7 cells were cultured through repeated passages at low density in standard DMEM medium lacking glucose (0 mg of glucose/L), and control DMEM medium (4500 mg of glucose/L). Cells were seeded at low density (2×10^5 cells/100 mm culture dish) in test media and allowed to expand until 80% confluent (approximately 20×10^6 cells/dish). Throughout each culture period, monolayers were monitored for changes in cell-cell interactions and cell morphology. A eukaryote expression plasmid containing the full α-catenin gene sequence[40] was transfected into L2a cells using Lipofectamine 2000 (Invitrogen, Carlsbad, CA). After transfection, cells were selected for Geneticin (G418; Invitrogen Canada Inc., Burlington, ON, Canada) antibiotic resistance and subcloned to produce clonal populations expressing α-catenin. Transfected cell lines were used for subsequent functional assays.

Western Blotting

Total protein from all parental cell lines (DLD-1, PC7, and L2A) and expression clones (D2, D4, D3, and G3) was obtained by cellular lysis using Cell Lysis Buffer (Cell Signaling Technology Inc., Danvers, MA) supplemented with aprotinin and phenylmethylsulfonyl fluoride after a brief wash in ice-cold PBS. Lysates were spun at $16,000 \times g$ for 20 minutes, and supernatant was stored at −80°C until analysis; 30 μg of total protein was loaded into 7.5% acrylamide gel and subjected to SDS-polyacrylamide gel electrophoresis. Proteins were transferred to polyvinylidene difluoride membranes (Roche Diagnostics, Indianapolis, IN) and blocked using 5% milk in Tris-buffered saline/Tween 20 for 1 hour at room temperature. Membranes were incubated in corresponding primary antibodies overnight at 4°C and then were washed and exposed to appropriate secondary antibodies for 30 minutes at room temperature. Primary antibodies used were rabbit anti-α-catenin (C-terminal specific, 1:5000; Sigma-Aldrich), rabbit anti-α1-catenin (N-terminal specific, 1:50,000; Epitome Biosystems, Inc., Waltham, MA), mouse anti-β-catenin (1:1000; BD Biosciences, San Jose, CA), rabbit anti-E-cadherin (1:1000; Cell Signaling Technology Inc.), and mouse anti-α-tubulin (1:200,000; Sigma-Aldrich). Junction and adhesion primary antibodies were obtained from BD Biosciences, and the dilutions used were as follows: mouse anti-desmoglein, 1:1000; mouse anti-N-cadherin, 1:2500; mouse anti-M-cadherin, 1:250; mouse anti-cadherin-5, 1:250; mouse anti-p120, 1:1000; mouse anti-E-cadherin, 1:2500; mouse anti-P-cadherin, 1:250; mouse anti-vinculin, 1:400; mouse anti-R-cadherin, 1:500; mouse anti-β-catenin, 1:500; mouse anti-γ-catenin, 1:200; mouse anti-fibronectin, 1:2500; mouse anti-β_4-integrin, 1:500; mouse anti-α_L-integrin, 1:5000; mouse anti-α_2-integrin, 1:250; mouse anti-α_5-integrin, 1:5000; mouse anti-α_3-integrin, 1:250; mouse anti-β_1-integrin, 1:2500; mouse anti-α_V-integrin, 1:250; mouse anti-β_3-integrin, 1:2500; and mouse anti-α-tubulin antibody, 1:40,000. Secondary antibodies used were anti-mouse peroxidase (1:20,000) and anti-rabbit peroxidase (1:10,000; both from Sigma-Aldrich). After extensive Tris-buffered saline/Tween 20 washes, membranes were exposed to chemiluminescence solution (Roche Diagnostics) (prepared according to kit instructions) and then visualized on X-ray film (Konica, Ramsey, NJ). Densitometric analysis was performed using ImageJ software.

Immunofluorescent Staining of Cultured Cells

Cells were grown to semiconfluence on positively charged glass slides in DMEM supplemented with 10% fetal bovine serum, Geneticin, and sodium pyruvate. Slides were removed, washed with ice-cold PBS for 5 minutes, dried, and fixed in 4% paraformaldehyde for 12 minutes at room temperature. Monolayers were permeabilized using 0.05% Tween 10 in PBS for 10 minutes, followed by blocking of unspecific binding with 10% normal goat serum in PBS for 1 hour at room temperature. Cells were incubated in rabbit anti-α-catenin primary antibody (1:200; Sigma-Aldrich) for 1 hour followed by goat anti-rabbit Cy3 secondary antibody (Jackson ImmunoResearch Laboratories Inc., West Grove, PA) in the dilution of 1: 200 for 30 minutes. Cells were incubated in anti-β-catenin primary antibody (1:200; BD Biosciences) for 1 hour followed by anti-mouse Alexa 488 secondary antibody (1:400; Molecular Probes, Eugene, OR) for 30 minutes. Cells were incubated in anti-E-cadherin primary antibody (1:100; Cell Signaling Technology Inc.) for 1 hour and subjected to goat anti-rabbit Cy3 secondary antibody (1:200; Jackson ImmunoResearch Laboratories Inc.) for 30 minutes. Cells were washed in PBS and counterstained with 4,6-diamidino-2-phenylindole (DAPI) (nuclear stain), and slides were mounted using Fluorescent Mounting Media (Dako, Carpenteria, CA). Cells not exposed to primary antibody were used as a negative control for secondary antibody. Images were captured at $\times$20 and $\times$100 objectives using QCapture software calibrated to a Leica DMLB microscope fitted with a Q imaging QICAM Fast1394 digital camera. Images obtained were merged using Adobe Photoshop 7.0 (Adobe Systems, Mountain View, CA). There was no detectable staining in the negative control.

In Vitro *Tumorigenicity Assays*

Soft agarose colony-forming efficiency was assessed by counting visible colonies produced after 15 days in soft agarose culture using a phase-contrast microscope at $\times$10 magnification and expressed as a percentage of cells plated.[41] Cells were resuspended in DMEM containing 20% fetal bovine serum, mixed 1:1 with molten 1% agarose to form a suspension of 0.5% agarose in complete medium, and layered into a six-well tissue culture dish precoated with 1 ml of 1% agarose to make a final concentration of 50 cells/cm^2. Complete culture medium (1 ml) was layered over the cross-linked matrix, and cultures were fed every 3 to 4 days by aspiration of medium and addition of 1 ml of complete culture medium.

The clonogenic survival after suspension was assessed by plating a single cell suspension (20 cells/cm^2) above cross-linked 1% agarose for 4 days and then transferring the medium-containing cells to an adherent plate. After 14 days, plates were washed with PBS and

Table 1. Summary of Xenograft Tissues Produced and Analyses Performed

Cells used in subcutaneous injection	Experiments performed on xenograft
PC7, L2a, 1:1 L2a:PC7 mixture	α-Catenin, CD31 immunostaining
DLD-1	Hoechst injection, α-catenin and nuclear staining
PC7, L2a	Xenograft growth
PC7, L2a	TUNEL labeling; Ki67 labeling
DLD-1, L2a, PC7, TD4, D3, G3	Xenograft growth

TUNEL, Terminal deoxynucleotidyl transferase dUTP nick-end labeling.

stained with 0.1% crystal violet in 20% methanol. Plates were randomized and scanned on a flatbed scanner, and the imaging program ImageJ was used to count the number of colonies per plate. Cells were plated in duplicate; adherent plates served as counting controls. Spheroid cultures were produced by layering a single cell suspension (33×10^3 cells/cm^2) above cross-linked 1% agarose in 96-well tissue culture plates. Subconfluent monolayers were treated for 2 hours with 10 μmol/L mitomycin C to arrest cell division and plated at a density of 1.67×10^3/cm^2 on either adherent tissue culture plastic or nonadherent 1% agarose substrate and monitored over 4 days in culture using the alamarBlue metabolic assay. alamarBlue is a cell viability indicator that relies on living cells to convert resazurin to the fluorescent molecule, resorufin.[42] Resazurin is a nontoxic, cell-permeable compound that is blue in color and virtually nonfluorescent. On entering cells, resazurin is reduced to resorufin, which produces bright red fluorescence.[43] The amount of fluorescence produced is proportional to the number of living cells.

In Vivo *Tumor Assays*

All *RAG1*$^{-/-}$ immune-deficient mice were housed in the Animal Care Isolation Facility at the University of Guelph. Mice were maintained under barrier conditions in cages of up to five mice per cage and were fed autoclaved chow and acid-treated water. Animal use was supervised by the University of Guelph local animal care committee in accordance with the guidelines of the Canadian Council on Animal Care. Xenografts were produced by s.c. injection of cells suspended in PBS containing 0.1% bovine serum albumin into the right flank region of mice sedated with 500 μl i.p. tribromoethanol (Avertin; Life Technologies, Inc., Carlsbad, CA).[44] For most experiments, 10^6 cells were injected; for xenografts produced from a mixed population of cells, a total of 4×10^6 cells were injected. Xenografts produced from mixed cell populations were produced by injection of a 1:1 ratio of PC7and L2a cells. Tumor volumes were calculated using the formula: (length × width^2 × 0.5)[45] and were monitored for 21 to 28 days after injection. Mice were then euthanized (CO_2 asphyxiation followed by cervical dislocation), and tumors were collected for further analysis; Table 1 summarizes xenografts produced and the analyses performed on the resulting tissues.

Cell sorting after Hoechst intravital labeling was performed using established methods.[46] In brief, DLD-1 parent xenografts were produced and intravital Hoechst dye was administered by tail vein injection. After 5 minutes, mice were euthanized and xenografts were dissected. Xenograft tissue was dissociated by both physical and enzymatic processing, and the cell suspension was sorted based on Hoechst 33342 fluorescence intensity on a single-excitation, dual-emission fluorescence-activated cell sorter (Photon Technology International, Brunswick, NJ). Cells from the lowest 6% of intensity were captured, cultured, and monitored for α-catenin expression and morphology.

Histology

Paraffin-embedded tissue fixed for 24 hours in 10% neutral buffered formalin was sectioned at 5 μm and mounted on Superfrost Plus slides. Sections were dewaxed, subjected to antigen retrieval (10 mmol/L citrate buffer, pH 6.0; microwaved for 8 minutes), equilibrated in PBS, and blocked using 5% bovine serum albumin in PBS. Sections were incubated with rabbit anti-α-catenin primary antibody (10% normal goat serum block, 1:400 for 30 minutes; 1:50 to 1:400 dilution, depending on the manufacturer's recommendations; Sigma-Aldrich) overnight at 4°C, followed by fluorescently tagged secondary antibody (1:400) for 1 hour at room temperature. Sections were stained with DAPI or propidium iodide (1 ng/ml for 1 minute) to produce nuclear counterstain and then were mounted in aqueous fluorescent mounting medium (Dako). Xenografts embedded in Cryomatrix were cut to 5-μm section thickness, fixed immediately for 15 minutes in AMRESCO's HistoChoice fixative (Mandel Scientific Company, Guelph, ON, Canada), and then immunostained as described previously. Labeling for each of the primary antibodies used in experiments was optimized for blocking reagent required, by titration of the antibody, and for primary antibody labeling time. Negative control sections using incubation buffer containing no primary antibody was used for each labeling replicate. Terminal deoxynucleotidyl transferase dUTP nick-end labeling of xenografts was performed using the protocol provided by the manufacturer (Roche Diagnostics). Cell counting and analysis were performed on two sections per xenograft, in a minimum of four xenografts per labeling protocol, using mid-tumor sections. Xenograft images were blindly randomized before counting and statistical analysis.

Determination of Vascular Endothelial Growth Factor Secretion (Enzyme-Linked Immunosorbent Assay)

For each cell line 500,000 cells were plated into 35-mm sterile culture dishes in DMEM containing 10% fetal bovine serum with gentamicin and sodium pyruvate and allowed to attach overnight. Cells were washed in PBS, and media were replaced by DMEM containing 2% fetal bovine serum. After 48 hours, conditioned media were

collected, centrifuged to remove dead cells, and stored at −80°C until use. Cells were trypsinized and counted for normalization purposes. The concentration of secreted vascular endothelial growth factor was measured using an enzyme-linked immunosorbent assay (R&D Systems, Minneapolis, MN) according to the manufacturer's conditions. Samples were run in duplicate, and two different replicates were included in the assay.

In Vivo *Angiogenesis Assay*

Mitomycin C-treated cells from the PC7 and L2a clones were mixed separately with BD Matrigel matrix and used to form subcutaneous plugs in *RAG1*$^{-/-}$ mice.[47] After 12 days *in vivo*, plugs were recovered, embedded in Cryomatrix, and snap-frozen in liquid N_2. Cryosections were cut, fixed, and labeled with the mouse endothelial cell marker isolectin GS-IB4 Alexa 488 (30 minutes 1:100; Dako)[45] and counterstained with DAPI. Slides were randomized, and the numbers of isolectin-positive blood vessel structures were counted in three separate areas of each section at ×10 magnification.

PCR Amplification and Sequences Analysis

Genomic DNA was isolated from cultured cells using an extraction kit (Qiagen, Hilden, Germany). Mutation analysis of codon Cyc767 of *CTNA1* (accession number NC_00005.8) was performed by amplification of the 480-bp fragment using the following primers: Cta forward 5′-GCCACACTGAACCTTTCAGAAA-3′ and Cta reverse 5′-GCCTTTCAGCCCTTGCAGT-3′. Mutations in codon 13 of *KRAS* (accession number NC_000012.10) were detected by amplification of 580-bp fragment using the following primers: Ras forward 5′-GAGTTTGTAAATGAAGTACAGTT-3′ and Ras reverse 5′-CTCTCACGAAACTCTGAAAT-3′.

PCR amplification was performed using Phusion high-fidelity DNA polymerase enzyme (New England Biolabs, Ipswich, MA) under the following conditions: one cycle at 98°C for 30 seconds, 35 cycles of 10 seconds at 98°C, 20 seconds at 64°C for *CTNA1*, 52°C for *KRAS,* and 20 seconds at 72°C, followed by a final cycle of 5 minutes at 72°C. PCR fragments were purified using GFX PCR DNA and a Gel Band Purification kit (GE Healthcare, Little Chalfont, Buckinghamshire, UK), and sequencing of each fragment in both directions was obtained.

Statistical Analysis

Analysis of variance tests were performed with the Tukey-Kramer multiple comparison test using GraphPad InStat software. The Bartlett statistic was used to verify that SDs were equal. Normality was tested using the Kolmogorov-Smirnov test. When only two means were being compared, a Student's *t*-test was used. All figures include SEM as error bars.

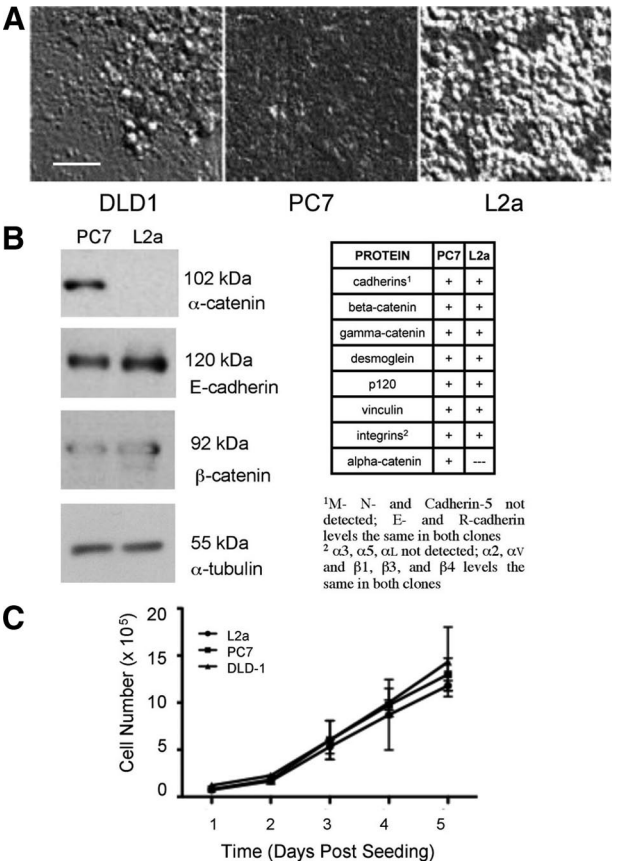

PROTEIN	PC7	L2a
cadherins[1]	+	+
beta-catenin	+	+
gamma-catenin	+	+
desmoglein	+	+
p120	+	+
vinculin	+	+
integrins[2]	+	+
alpha-catenin	+	---

[1]M- N- and Cadherin-5 not detected; E- and R-cadherin levels the same in both clones
[2] α3, α5, αL not detected; α2, αV and β1, β3, and β4 levels the same in both clones

Figure 1. Morphological differences between clones of DLD-1 colorectal carcinoma cells. **A:** DLD-1 cells display variable cell-cell and cell-matrix adhesion characteristics, as revealed by differential interference contrast microscopy. Clone PC7 forms a tightly compacted monolayer with indistinct cell-cell boundaries, whereas clone L2a cells display a "rounding" phenotype, with a less compact layer on the culture dish, covered by patches of multilayered clusters of weakly adherent cells. DLD-1 parental cultures are a mixture of both morphologies. **B:** Expression of proteins associated with cell-cell and cell-matrix adhesion was evaluated by Western blotting. In all of the proteins examined, the only quantitative difference between PC7 and L2a was that the later clone was negative for the adherence junction protein α-catenin. **C:** Despite the obvious variation in cell morphology, no significant differences were seen in cell proliferation between DLD-1 parent cells or either clone. Scale bar = 50 μm.

Results

We used a fluorescence-based technique[46] to obtain cells from ischemic regions of xenografts generated from the DLD-1 colorectal cancer cell line and found that the previously reported α-catenin-negative round cell phenotype was highly enriched in poorly perfused regions of these tumors. To explore the impact of these cells on tumorigenicity and the influence of ischemia on the generation of this phenotype, we used serial dilution to produce DLD-1 subclones with either epithelial or rounding cell morphologies. One clone of each epithelial (PC7) and rounding (L2a) subtype was used for the ensuing studies (Figure 1A). Because of differences in morphology between PC7 and L2a and based on previous reports that DLD-1 was heterogeneous with respect to α-catenin expression, we performed Western blots on cell lysates to evaluate the expression of adhesion-related proteins. With the exception of α-catenin, all other

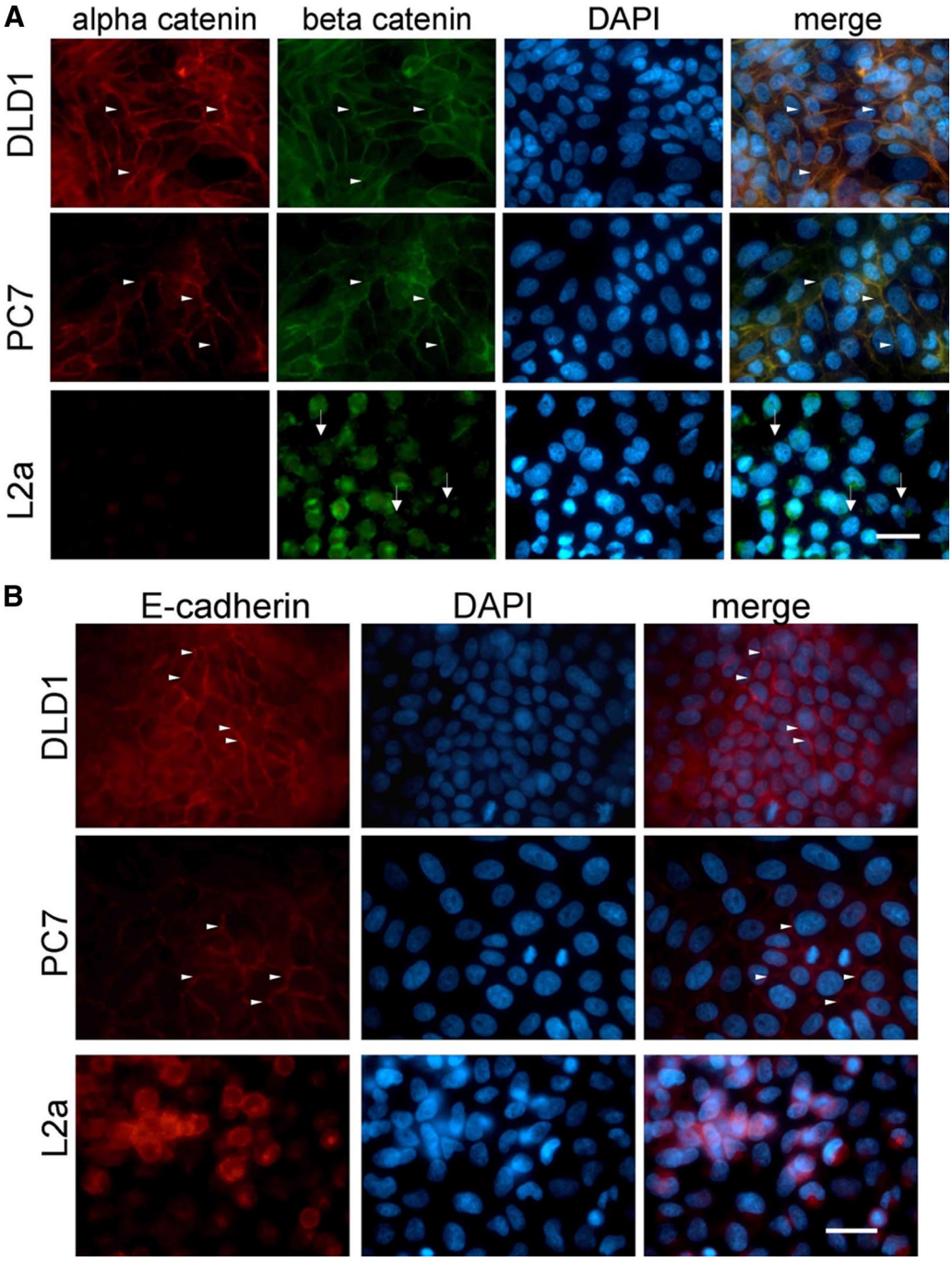

Figure 2. Immunofluorescence of cultured monolayers immunostained for α-catenin, β-catenin, and E-cadherin. **A:** The DLD-1 parent and PC7 clone show extensive α-catenin and β-catenin immunostaining, localized to cell-cell junctions (**arrowheads**). L2a cells lack detectable α-catenin, and their β-catenin is disorganized and primarily cytosolic (**arrows**). Merged images show colocalization of α- and β-catenin as yellow fluorescence. A DAPI counterstain was used to identify cellular nuclei. Scale bar = 50 μm. **B:** The DLD-1 parent and PC7 cells express E-cadherin at cell-cell junctions (**arrowheads**), whereas L2a cells have dispersed E-cadherin. A DAPI counterstain was used to identify cellular nuclei. Scale bar = 50 μm.

proteins evaluated were not differentially expressed between these clones (Figure 1B). Furthermore, immunofluorescent labeling of cultured PC7 and L2a cells showed no qualitative differences in β-catenin protein localization, whereas E-cadherin labeling was diffuse on the loss of α-catenin (Figure 2, A and B). We confirmed by direct DNA sequencing that the L2a clone is homozygous for a premature opal stop mutation (C → A transversion) at Cys767 (Table 2), as has been reported.[31] Also as reported previously,[37,38] DLD-1 and its derivatives are mutant for *KRAS* at codon 13. Statistical analysis of the monolayer cycling rate showed no differences between the DLD-1 parental, PC7, and L2a cell lines (Figure 1C).

To study the role of α-catenin in CRC cells we re-expressed it in the L2a subclone cells by stable transfection with an expression vector. We then verified the different effects of α-catenin-expressed protein on cell survival, morphology, and tumorigenicity. Western blot-

Table 2. Mutation Status of DLD-1 Cells and Derivatives

Cell line	*KRAS* codon 13	*CTNNA1* codon 767
DLD-1 (parent)	mut GGC:GAC	wt TGC
PC7	mut GGC:GAC	wt TGC
L2a	mut GGC:GAC	mut TGC:TGA
a-Catenin expression clone D3	mut GGC:GAC	wt TGC
α-Catenin expression clone G3	mut GGC:GAC	wt TGC
α-Catenin expression clone TD2	mut GGC:GAC	wt TGC
α-Catenin expression clone TD4	mut GGC:GAC	wt TGC

mut, mutation, wt, wild type.
Underline indicates substituted nucleotide in mutant condon.

Table 3. *In Vitro* Assays of Tumorigenicity

Cell line	Soft agarose colony formation	Clonogenic survival	Survival in suspension
DLD-1	4.5 (0.03)	43.6 (4.91)	35.6 (5.90)*
L2a	7.9 (0.25)†	81.0 (2.96)‡	79.9 (5.65)
PC7	1.3 (0.15)	32.8 (4.18)	14.1 (5.83)*
D3	8.0 (0.33)†	77.6 (1.35)‡	77.9 (6.40)
TD2	3.1 (1.25)	45.5 (1.42)	53.6 (3.00)
TD4	1.8 (0.42)	36.3 (2.93)	61.1 (11.8)
G3	1.9 (0.78)	38.3 (1.85)	60.2 (4.81)

Data are mean (SEM).
*Significantly different survival in suspension from all other cell lines but not from each other ($P < 0.001$).
†Significantly different colony formation from all other cell lines but not from each other ($P < 0.001$).
‡Significantly different clonogenic survival from all other cell lines but not from each other ($P < 0.001$).

ting for α-catenin (Figure 3A) revealed that three L2a-derived clones (TD2, TD4, and G3) produced an intermediate level of α-catenin and one clone (D3) produced no detectable α-catenin (and thus acted as a negative control for transfection in subsequent experiments). Re-introduction of the *CTNNA1* gene resulted in re-establishment of an intact epithelial monolayer (Figure 3B), although the intermediate levels of α-catenin expressed by these transfected cells were insufficient to fully restore cell-cell adhesion characteristics to all cells of the monolayer. Sequence analysis indicates that four clones of L2a transfected with expression constructs for full-length α-catenin protein are genotypically wild type, because of integration of the construct DNA, although phenotypically they express variable amounts of α-catenin protein; these four clones are also mutant *KRAS* (Table 2). Western blots for β-catenin and E-cadherin in DLD-1 derivatives and α-catenin re-expression clones demonstrate no significant loss of other elements of the adhesion junction complex (Figure 3C).

The soft agarose colony formation assay[48] showed reduced cellular tumorigenic ability when α-catenin protein was present (Table 3). When measured by the ability of cells to form adherent colonies after suspension, α-catenin protein likewise reduced clonogenic ability (Table 3). Assessment of metabolic activity in suspension but in the presence of cell-cell contact showed that α-catenin also modulates cellular metabolism independently of mitosis (Table 3).

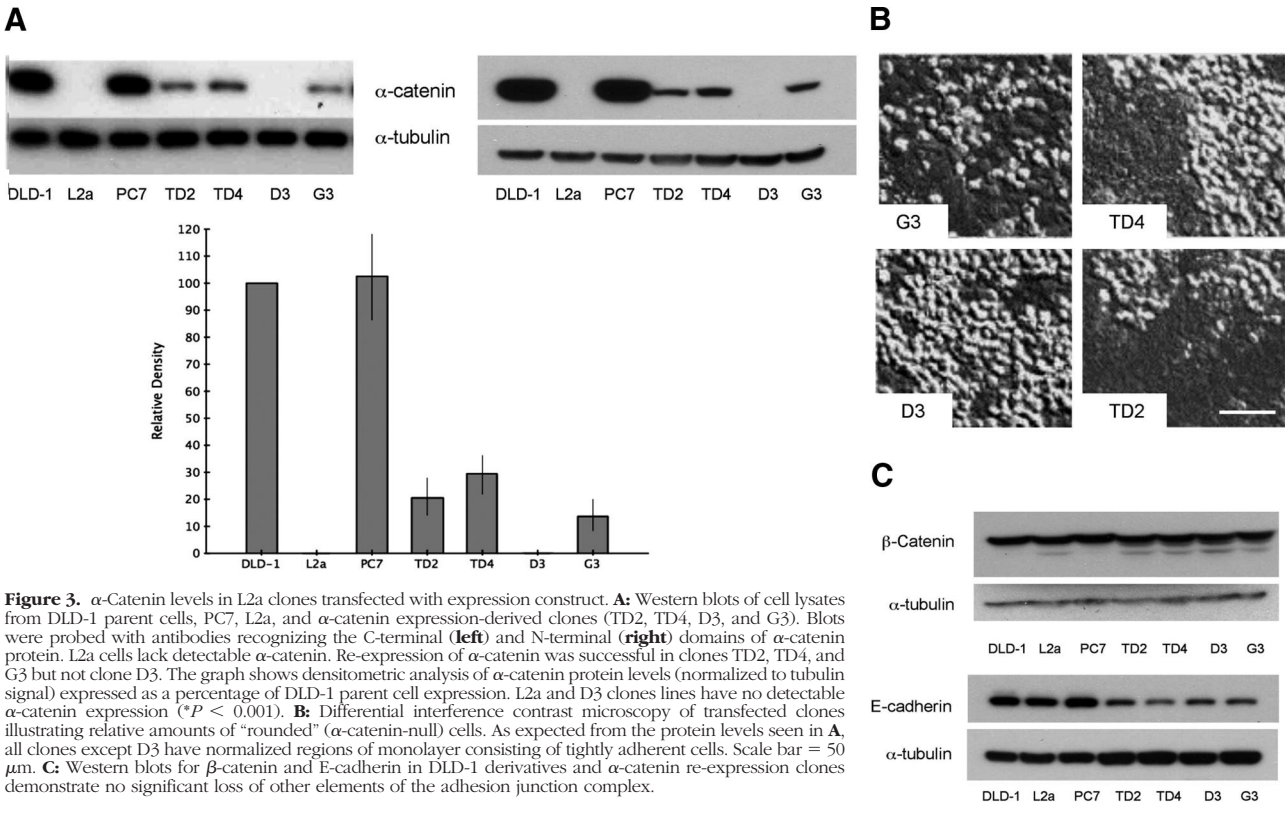

Figure 3. α-Catenin levels in L2a clones transfected with expression construct. **A:** Western blots of cell lysates from DLD-1 parent cells, PC7, L2a, and α-catenin expression-derived clones (TD2, TD4, D3, and G3). Blots were probed with antibodies recognizing the C-terminal (**left**) and N-terminal (**right**) domains of α-catenin protein. L2a cells lack detectable α-catenin. Re-expression of α-catenin was successful in clones TD2, TD4, and G3 but not clone D3. The graph shows densitometric analysis of α-catenin protein levels (normalized to tubulin signal) expressed as a percentage of DLD-1 parent cell expression. L2a and D3 clones lines have no detectable α-catenin expression (*$P < 0.001$). **B:** Differential interference contrast microscopy of transfected clones illustrating relative amounts of "rounded" (α-catenin-null) cells. As expected from the protein levels seen in **A**, all clones except D3 have normalized regions of monolayer consisting of tightly adherent cells. Scale bar = 50 μm. **C:** Western blots for β-catenin and E-cadherin in DLD-1 derivatives and α-catenin re-expression clones demonstrate no significant loss of other elements of the adhesion junction complex.

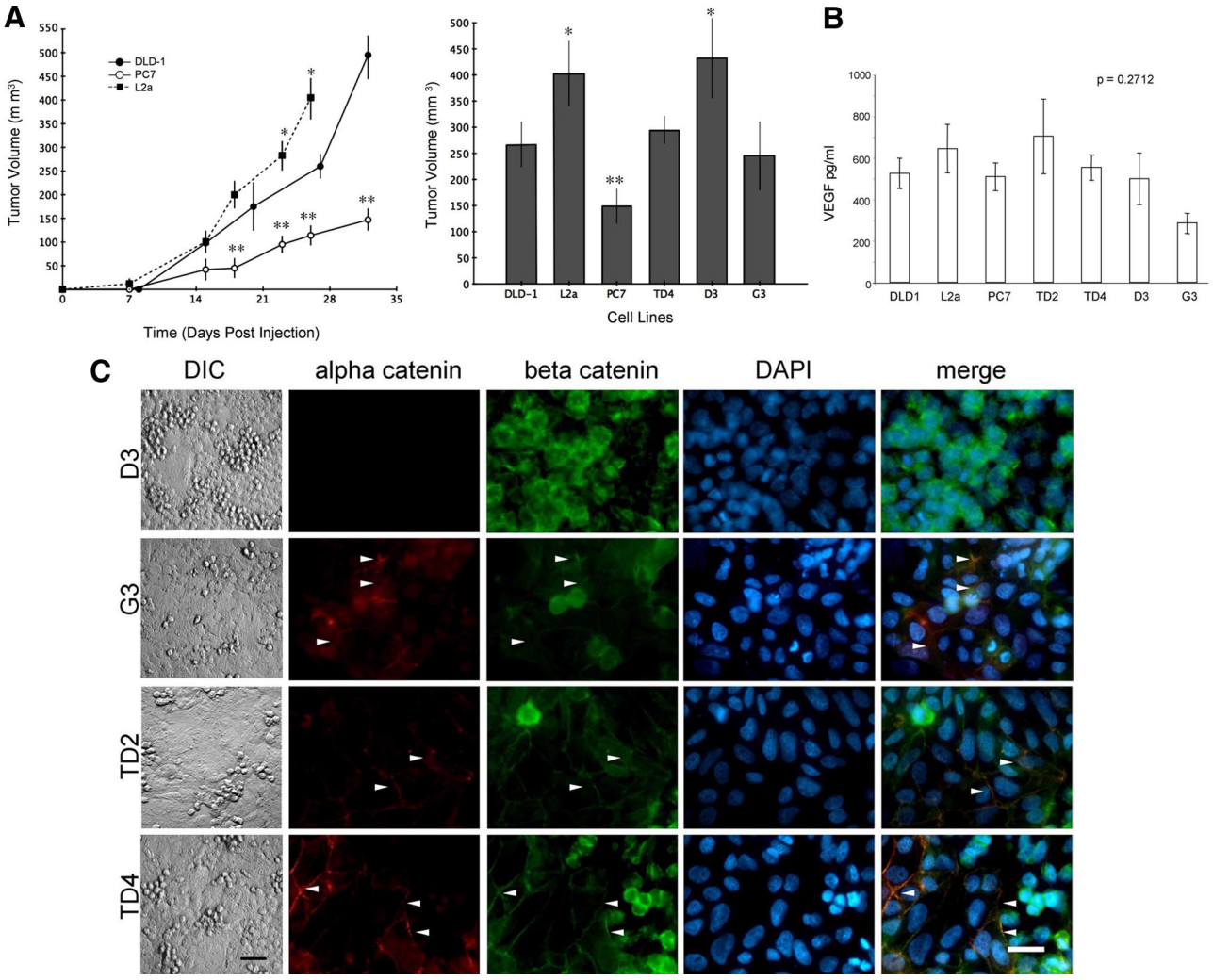

Figure 4. Influence of α-catenin expression on tumor growth *in vivo*. **A:** PC7 xenografts grow significantly slower than either DLD-1 parent tumors or L2a cells when grafted s.c. into the flank of immune-deficient mice (**$P < 0.05$). L2a and D3 clones showed statistically increased tumor volume growth at day 25 compared with PC7 (*$P < 0.05$). DLD-1 parent and other clones show no significant differences from each other. **B:** Production of the angiogenic factor vascular endothelial growth factor (VEGF), as detected by enzyme-linked immunosorbent assay, did not differ significantly between the parental cell lines or the clones ($P = 0.2712$). **C:** Immunofluorescence of α-catenin expression clones immunostained for α-catenin, β-catenin, and DAPI nuclear counterstain. Differential interference contrast (DIC) images on the **left** show the morphology of the cell monolayers. All clones except D3 show normalization of the monolayer, with increased areas of adherent monolayer and tight cell-cell boundaries and fewer cells with the "rounding" phenotype. Concomitant with this, all clones except D3 express detectable levels of α-catenin, and the majority of cells have relocalized both α-catenin and β-catenin to cell-cell adhesion points (**arrowheads**). In contrast, D3 cells retain the disrupted β-catenin localization of their parent L2a. Scale bars = 50 μm.

L2a cells grew as xenografted tumors in immune-deficient mice more quickly than PC7 cells (Figure 4A). Hematoxylin and eosin staining of xenografts indicated that PC7 tumors had larger total necrotic areas (as a proportion of section area) than xenografts produced from L2a cells (data not shown). Both terminal deoxynucleotidyl transferase dUTP nick-end labeling and Ki-67 rates were also significantly higher for the L2a tumors than for the PC7 tumors (Table 4). Recruitment of neovasculature into a subcutaneous Matrigel implant demonstrated no altered angiogenic capacity because of the α-catenin status of these cells (Table 4), a property supported by the lack of significant differences in vascular endothelial growth factor secretion between cells with various α-catenin levels (Figure 4B). Together, these results suggest that the L2a clone was able to overcome tumor formation barriers more easily than the PC7 clone. Xenografted TD4 and G3 cells had growth rates similar to those of the DLD-1 parent cells, in keeping with their intermediate levels of expression of α-catenin (Figures 3B and 4C). In contrast, the D3 clone, with no detectable α-catenin protein, showed accelerated growth, comparable with that of xenografted L2a cells (Figure 4, A and C). In combination with the *in vitro* clonogenic results, these results suggest that the L2a clone lacking α-catenin was able to establish and maintain tumors more easily than the PC7 clone expressing the protein.

α-Catenin-negative subpopulations of the DLD-1 parent cell line were enriched in the ischemic microenvironment within xenografts. Using the Hoechst intravital labeling method described previously[39,46,49] xenograft cells were stained *in vivo*, sorted on the basis of their proximity to patent vasculature and cultured. Cells obtained from the least perfused regions of tumors were

Table 4. Proliferation and Angiogenic Characteristics of Xenografts from α-catenin-expressing and -null Cells *In Vivo*

Cell line	Ki67 staining	TUNEL staining	Blood vessel density
PC7	58.6 (1.17)*	5.50 (0.20)*	58.0 (7.7)†
L2a	73.5 (0.80)	8.33 (0.65)	57.2 (6.4)†

Data are mean (SEM) Ki 67 staining indicates Ki67-positive cells in xenograft tumors. TUNEL staining indicates TUNEL-positive cells/field in xenograft tumors. Blood vessel density indicates blood vessel number/×10 field in s.c. implanted Matrigel pellets containing tumor cells.

*Statistically significant from L2a ($P < 0.001$).

†Both cell lines recruited significantly more blood vessels than cell-free Matrigel (38.3 [9.4]/×10 field; $P < 0.001$).

almost entirely α-catenin-negative, whereas cells isolated from well perfused portions of xenografts were primarily α-catenin-positive. Cells that were α-catenin-negative yet apparently viable (as indicated by their intact, uncondensed nuclei) were found in poorly perfused areas identified by intravital Hoechst dye within intact xenografts (Figure 5, A–D). Dual labeling for α-catenin and CD31 (endothelial marker anti-platelet-endothelial cell adhesion molecule) showed that cells expressing α-catenin preferentially clustered next to CD31-positive blood vessels in intact xenografts generated from mixtures of PC7 and L2a cells (Figure 6, A–I), consistent with our results from cell sorting of dispersed DLD-1 tumors.

We explored possible mechanisms associated with this selective location in tumors of α-catenin-null cells by exposing PC7 (which expresses α-catenin and forms a tightly adhesive monolayer *in vitro*) to culture conditions

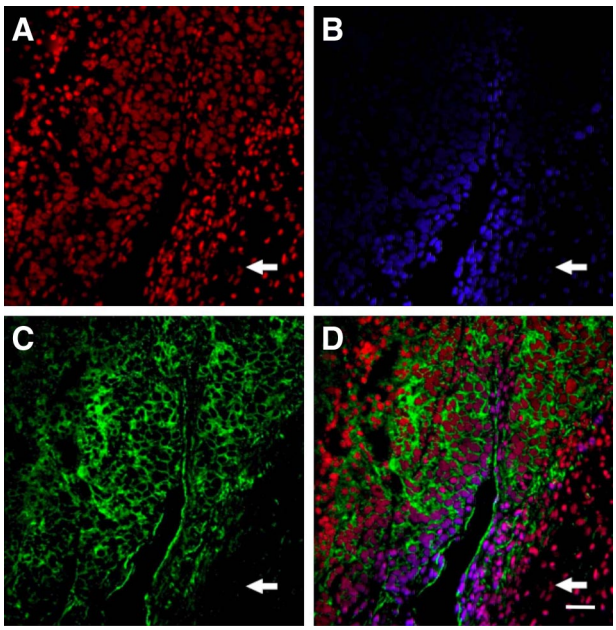

Figure 5. α-Catenin-expressing cells are preferentially located in well perfused regions of xenografts. DLD-1 xenograft section counterstained with propidium iodide to show nuclei (red; **A**), immunostained for α-catenin (green; **B**) and showing Hoechst fluorescence indicating region of perfusion (blue; **C**). **D:** Merging of three fluorescent channels. Cells lacking α-catenin expression located in nonperfused areas are indicated (**white arrow**). Scale bar = 25 μm.

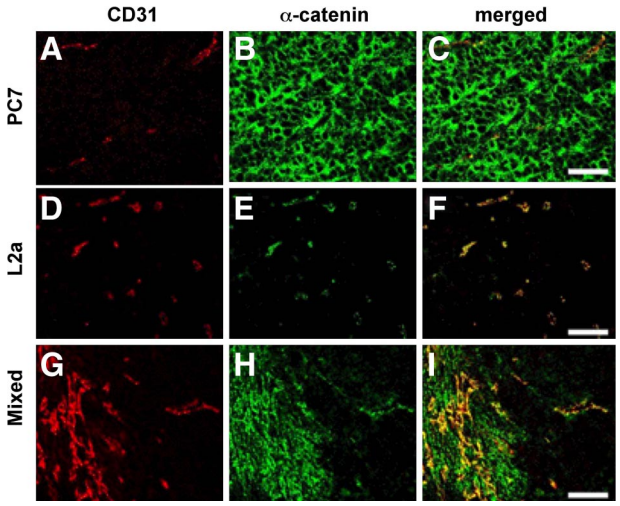

Figure 6. α-Catenin expression in xenografts made from PC7, L2a, and mixed clones. **A–C:** Representative xenografts immunolabeled for endothelial cells (CD31, red) and α-catenin (green) and composite images (merged). PC7 cells produce well vascularized xenografts with α-catenin labeling throughout the tissue. **D–F:** L2a cells produce xenografts with α-catenin-positive endothelial cells, but α-catenin-negative cancer cells. **G–I:** Xenografts produced from a 50:50 mixture of PC7 and L2a cells produce tumors that contain α-catenin-positive cancer cells preferentially located around the blood vessels. Scale bar = 50 μm.

mimicking tumor ischemia. Prolonged culture in glucose-free media accelerated the spontaneous loss of α-catenin protein: after approximately 20 population doublings under glucose deprivation, PC7 cultures began to show patches of cells in the monolayer indicative of the rounding phenotype (Figure 7, A–C). We confirmed their α-catenin-negative status by immunostaining and Western blotting and DNA sequence of the premature stop codon in their *CTNNA1* gene (Figure 7, D–H). PC7 cells cultured under identical conditions but in the presence of glucose underwent greater than 60 population doublings before such morphological changes became apparent. Together these findings suggest that spontaneous loss of α-catenin protein expression may occur in ischemic regions of solid tumors, leading to enhanced cell survival and subsequent tumor progression.

Discussion

Using a combination of approaches, we demonstrated that α-catenin acts as a potent tumor suppressor in colorectal carcinoma cells. Reintroduction of α-catenin into null cells decreased tumorigenic ability *in vitro* and *in vivo*. Cells lacking α-catenin were preferentially located in ischemic regions of xenografts produced from mixed populations of cells. Exposure of α-catenin-expressing cells to ischemia-related conditions *in vitro* (hypoglycemia) demonstrated that stressful microenvironments contribute to this α-catenin loss. These results illustrate that the tumor environment affects the expression of this tumor suppressor protein and that the lack of α-catenin directly affects the tumorigenicity of CRC cells.

The DLD-1 cell line was initially derived from an adenocarcinoma of sporadic origin[32] and has been extensively studied for its heterogeneous cellular makeup[30,32,50,51]; it is

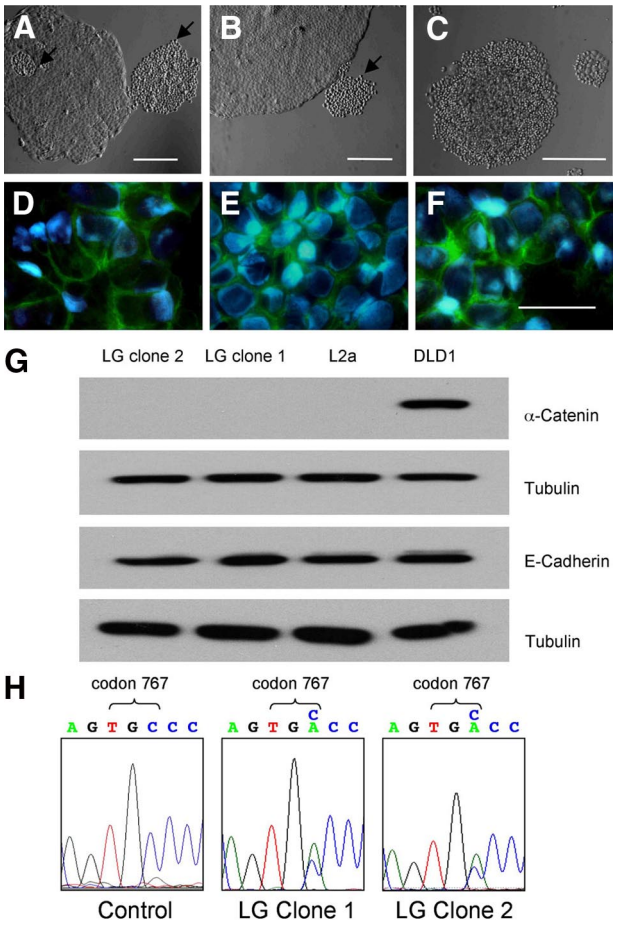

Figure 7. Prolonged exposure of PC7 cells *in vitro* to hypoglycemic conditions gives rise to α-catenin-null cells. **A:** Differential interference contrast micrographs of PC7 monolayer with areas of transition to rounding morphology (**black arrows**) after sustained culture (20 population doublings) in glucose-free medium. **B:** PC7 cells in cultured in glucose-containing medium for extensive periods of time (60 population doublings) also give rise to cells with rounding morphology but much less frequently (**black arrow**). **C:** Rounding morphology of cells derived from low glucose culture is stable, as shown by colonies of such cells now growing in glucose-containing medium. **D–F:** Three different rounded clones of PC7 cells generated by low glucose exposure lack detectable α-catenin protein (red) and have disrupted β-catenin staining expression patterns (green; DAPI counterstain for nuclei). Scale bars = 50 μm. **G:** Western blot demonstrates no detectable α-catenin in cells derived from low glucose selection of PC7 cells (LG clones 1 and 2); E-cadherin expression was not altered in these clones. **H:** Sequence analysis of two colonies from low glucose selection reveals mutations in codon 767 of the α-catenin gene, generating a premature stop codon.

one of a group of cell lines (DLD-1, HCT-15, HCT-8, and HRT-18) derived from the same patient.[33] Previous studies using a DLD-1 subclone lacking α-catenin demonstrated that reintroduction of α-catenin results in reduced proliferation and altered adhesion in three-dimensional conditions.[28] We show here that α-catenin is also able to modulate the tumorigenic potential of the DLD-1 cells *in vivo*, implying that α-catenin may act as a brake on the aggressive behavior of the *KRAS*^{G13D} oncogene expressed by these cells. Point mutations in the *KRAS* gene occur early in the development of colorectal neoplasms and are found in 35 to 50% of colorectal adenomas and cancers. Disrupting the mutant *KRAS* gene in DLD-1 cells by homologous recombination resulted in a cell line expressing only wild-type *KRAS* that had altered morphology and reduced capacity for anchorage-independent growth and tumorigenicity.[37] The original *KRAS* mutation was probably directly responsible for the malignant phenotype of the DLD-1 cells because a coexisting mutation in the *P53* gene was not sufficient to produce tumors in cells lacking KRAS^{G13D} mutant protein.[37] Our findings of a differential effect of α-catenin loss on cells that are *KRAS* mutants suggests that α-catenin levels are able to modify the effects of KRAS signaling, which is a novel role for α-catenin in tumorigenesis.

Uncoupling of α-catenin from β-catenin by expression of a dominant-negative form of the α-catenin phosphorylating protein SHP2 leads to disruption of adherens junction formation in NIH-3T3 cells,[29] resulting in increased growth attributed to β-catenin nuclear translocation and activation of the β-catenin-TCF/LEF signaling pathway.[29] Therefore, α-catenin uncoupling regulates cell-cell contact and can lead to downstream β-catenin signaling. The α-catenin regulator SHP2 also increases the half-life of activated Ras (GTP-Ras) by obstructing its inactivation catalyzed by the Ras GTPase-activating protein (Ras-GAP).[52] These results support the idea that α-catenin functions to sequester β-catenin and its downstream signaling but also indicates cross talk between α-catenin-mediated adherens junction control and normal Ras activity. Although KRAS^{G13D} codes for a constitutively active protein, signaling by coexisting wild-type protein may exert some control over cellular processes when α-catenin is present. Disruption of α-catenin and its loss may lead to altered signaling because of cellular conformation changes and a loss of cellular growth control in three-dimensional growth conditions.

Development of a rounding cell phenotype as a result of disrupted E-cadherin-mediated adhesion is common in colorectal cancer. Vécsey-Semjén et al[53] characterized eight novel, low-passage colorectal cancer cell lines exhibiting alterations in junctional proteins, mesenchymal markers, and deregulated signaling cascades. Interestingly, cell lines isolated from primary tumors and bearing a rounding morphology had defects in their adhesion junctions, including low E-cadherin expression and α-catenin loss. This finding illustrates that primary cells isolated from tumors exhibit the rounding behavior and that this phenotype is linked to α-catenin loss. A similar "epithelial to round" transition occurs in human colorectal cancer LoVo cells modulated by plakoglobin expression[54] is also associated with the acquisition of increased cellular replication and motility.

Adherens junctions were incomplete in our L2a cells, apparently because of a lack of α-catenin. Using antibodies specific to either the N-terminal or C-terminal domains of α-catenin, we confirmed that loss of α-catenin protein, rather than expression of a truncated form, occurred in these cells. In both PC7 and L2a cells, β-catenin maintained a diffuse localization with no differential nuclear labeling; hence, differential activation of the β-catenin/LEF signaling cascade is probably not responsible for the altered cell parameters we observed. We showed that even the partial re-expression of α-catenin protein in null L2a cells reduced their ability to survive in suspension, form colonies in soft agarose, and generate tumors in immune-deficient mice. Similar to what we observed

here, transfection of α-catenin into PC9 lung carcinoma cells lacking α-catenin resulted in the reformation of E-cadherin junctional complexes and repolarization.[26] Reintroduction of α-catenin into an ovarian carcinoma-derived cell line also attenuated the ability of these cells to produce tumors in nude mice.[23]

Differential tumor growth rates in our study were apparently not due to increased angiogenesis or reduced apoptosis in xenografts generated from α-catenin-null cells. Although *in vitro* cell proliferation rates were not altered by α-catenin status, L2a tumors displayed an approximately 25% higher mitotic index (as determined by Ki-67 staining) than PC7 xenografts, suggesting that higher *in vivo* proliferation rates may account for the increased tumor volumes. In mixed tumors, α-catenin-expressing cells were preferentially located next to blood vessels, supporting the idea that loss of α-catenin allowed cells to survive and proliferate in harsher microenvironments within the tumor. The larger proportion of necrotic areas in xenografts produced from PC7 cells versus L2a cells, coupled with the preferential localization of α-catenin-null cells in regions distal from perfused blood vessels also suggests that such cells have a selective survival and/or growth advantage in marginal environments. This effect could be attributed to increased vascularization; however, L2a and PC7 cells had no distinguishable difference in angiogenic parameters.

It is also possible that α-catenin was preferentially lost in the nutrient-depleted ischemic environment of the xenografts. Approximately 90% of human colorectal tumors associated with hereditary nonpolyposis colorectal cancer show microsatellite instability and DNA mismatch repair deficiency, which accounts for up to 15% of sporadic colorectal, endometrial, and other cancers.[55] The DLD-1 cell line harbors biallelic nonsense mutations in the *hMSH6* gene but retains activity of hMLH1 and hMSH2 proteins.[56,57] In addition, *MRE11* (which functions in double-stranded break repair) is heterozygously mutated[58] and *P53* is mutated in both alleles.[34] The human α-catenin (*CTNNA1*) gene contains at least one microsatellite region.[59] The sister cell lines DLD-1 and HCT-8 are susceptible to the loss of α-catenin protein expression because they already possess one mutated *CTNNA1* gene and are microsatellite instability-high.[33,35] Further mutation or exon skipping in the second allele of *CTNNA1* in HCT-8 cells produced a premature stop codon.[60] Disruption of *CTNNA1* by frameshift and other mutations has also been reported in PC9 lung carcinoma and PC3 prostate carcinoma cell.[61,62] In clinical cases of colon cancer, internal deletion resulted in production of a truncated α-catenin protein.[40,63] Frameshift mutations were also responsible for DLD-1 α-catenin protein loss,[63] and we confirmed that our L2a cells are also homozygous mutant for *CTNNA1*.

When DLD-1 cells are exposed to ischemic conditions *in vitro* and *in vivo*, they down-regulated their mismatch repair protein MSH2, with concomitant generation of point mutations in *KRAS*.[38] We hypothesized that α-catenin mutation might also occur in PC7 clones exposed to similar environmental conditions. Because hypoglycemia was a more potent inducer of MSH2 reduction than hypoxia,[38] we explored how glucose deprivation influenced α-catenin levels in this present study and found accelerated loss of α-catenin. Reinstating hMSH6 into HCT-8 prevented the frequent inactivation of the α-catenin gene,[35] showing that MSH6 function is responsible for α-catenin loss in the HCT-8 cell line. An analogous process may be occurring in our PC7 cells, highlighting the role of stressful tumor environments in driving mutation events involving inactivation of a tumor suppressor gene and subsequent cancer progression.

Acknowledgments

Dr. David Rimm, Yale University School of Medicine, generously provided the α-catenin expression plasmid used in this study. We are also grateful for the excellent animal husbandry of Ms. Barb Mitchell, and the technical assistance and advice of other members of the Coomber Laboratory.

References

1. Fearon ER, Vogelstein B: A genetic model for colorectal tumorigenesis. Cell 1990, 61:759–767
2. Nicolson GL: Generation of phenotypic diversity and progression in metastatic tumor cells. Cancer Metastasis Rev 1984, 3:25–42
3. Perl AK, Wilgenbus P, Dahl U, Semb H, Christofori G: A causal role for E-cadherin in the transition from adenoma to carcinoma. Nature 1998, 392:190–193
4. Wijnhoven BP, Dinjens WN, Pignatelli M: E-cadherin-catenin cell-cell adhesion complex and human cancer. Br J Surg 2000, 87:992–1005
5. Zavadil J, Bottinger EP: TGF-β and epithelial-to-mesenchymal transitions. Oncogene 2005, 24:5764–5774
6. Thiery JP, Sleeman JP: Complex networks orchestrate epithelial-mesenchymal transitions. Nat Rev Mol Cell Biol 2006, 7:131–142
7. Furukawa Y, Nakatsuru S, Nagafuchi A, Tsukita S, Muto T, Nakamura Y, Horii A: Structure, expression and chromosome assignment of the human catenin (cadherin-associated protein) α 1 gene (CTNNA1). Cytogenet Cell Genet 1994, 65:74–78
8. McPherson JD, Morton RA, Ewing CM, Wasmuth JJ, Overhauser J, Nagafuchi A, Tsukita S, Isaacs WB: Assignment of the human α-catenin gene (CTNNA1) to chromosome 5q21–q22. Genomics 1994, 19:188–190
9. Nollet F, van Hengel J, Berx G, Molemans F, van Roy F: Isolation and characterization of a human pseudogene (CTNNAP1) for αE-catenin (CTNNA1): assignment of the pseudogene to 5q22 and the αE-catenin gene to 5q31. Genomics 1995, 26:410–413
10. Drees F, Pokutta S, Yamada S, Nelson WJ, Weis WI: α-Catenin is a molecular switch that binds E-cadherin-β-catenin and regulates actin-filament assembly. Cell 2005, 123:903–915
11. Pokutta S, Drees F, Yamada S, Nelson WJ, Weis WI: Biochemical and structural analysis of α-catenin in cell-cell contacts. Biochem Soc Trans 2008, 36:141–147
12. Kobielak A, Pasolli HA, Fuchs E: Mammalian formin-1 participates in adherens junctions and polymerization of linear actin cables. Nat Cell Biol 2004, 6:21–30
13. Pappas DJ, Rimm DL: Direct interaction of the C-terminal domain of α-catenin and F-actin is necessary for stabilized cell-cell adhesion. Cell Commun Adhes 2006, 13:151–170
14. Scholten AN, Aliredjo R, Creutzberg CL, Smit VT: Combined E-cadherin, α-catenin, and β-catenin expression is a favorable prognostic factor in endometrial carcinoma. Int J Gynecol Cancer 2006, 16:1379–1385
15. Nelson WJ, Nusse R: Convergence of Wnt, β-catenin, and cadherin pathways. Science 2004, 303:1483–1487

16. Reya T, Clevers H: Wnt signalling in stem cells and cancer. Nature 2005, 434:843–850
17. Yan HX, Yang W, Zhang R, Chen L, Tang L, Zhai B, Liu SQ, Cao HF, Man XB, Wu HP, Wu MC, Wang HY: Protein-tyrosine phosphatase PCP-2 inhibits β-catenin signaling and increases E-cadherin-dependent cell adhesion. J Biol Chem 2006, 281:15423–15433
18. Gottardi CJ, Gumbiner BM: Distinct molecular forms of β-catenin are targeted to adhesive or transcriptional complexes. J Cell Biol 2004, 167:339–349
19. Kang Y, Massague J: Epithelial-mesenchymal transitions: twist in development and metastasis. Cell 2004, 118:277–279
20. Vasioukhin V, Bauer C, Degenstein L, Wise B, Fuchs E: Hyperproliferation and defects in epithelial polarity upon conditional ablation of α-catenin in skin. Cell 2001, 104:605–617
21. Chan EF, Gat U, McNiff JM, Fuchs E: A common human skin tumour is caused by activating mutations in β-catenin. Nat Genet 1999, 21:410–413
22. Gat U, DasGupta R, Degenstein L, Fuchs E: De Novo hair follicle morphogenesis and hair tumors in mice expressing a truncated β-catenin in skin. Cell 1998, 95:605–614
23. Bullions LC, Notterman DA, Chung LS, Levine AJ: Expression of wild-type α-catenin protein in cells with a mutant α-catenin gene restores both growth regulation and tumor suppressor activities. Mol Cell Biol 1997, 17:4501–4508
24. Hirano S, Kimoto N, Shimoyama Y, Hirohashi S, Takeichi M: Identification of a neural α-catenin as a key regulator of cadherin function and multicellular organization. Cell 1992, 70:293–301
25. Shimoyama Y, Nagafuchi A, Fujita S, Gotoh M, Takeichi M, Tsukita S, Hirohashi S: Cadherin dysfunction in a human cancer cell line: possible involvement of loss of α-catenin expression in reduced cell-cell adhesiveness. Cancer Res 1992, 52:5770–5774
26. Watabe M, Nagafuchi A, Tsukita S, Takeichi M: Induction of polarized cell-cell association and retardation of growth by activation of the E-cadherin-catenin adhesion system in a dispersed carcinoma line. J Cell Biol 1994, 127:247–256
27. Van Hoorde L, Pocard M, Maryns I, Poupon MF, Mareel M: Induction of invasion in vivo of α-catenin-positive HCT-8 human colon-cancer cells. Int J Cancer 2000, 88:751–758
28. Matsubara S, Ozawa M: Expression of α-catenin in α-catenin-deficient cells results in a reduced proliferation in three-dimensional multicellular spheroids but not in two-dimensional monolayer cultures. Oncogene 2004, 23:2694–2702
29. Burks J, Agazie YM: Modulation of α-catenin Tyr phosphorylation by SHP2 positively effects cell transformation induced by the constitutively active FGFR3. Oncogene 2006, 25:7166–7179
30. Dexter DL, Spremulli EN, Fligiel Z, Barbosa JA, Vogel R, VanVoorhees A, Calabresi P: Heterogeneity of cancer cells from a single human colon carcinoma. Am J Med 1981, 71:949–956
31. Vermeulen SJ, Bruyneel EA, Bracke ME, De Bruyne GK, Vennekens KM, Vleminckx KL, Berx GJ, van Roy FM, Mareel MM: Transition from the noninvasive to the invasive phenotype and loss of α-catenin in human colon cancer cells. Cancer Res 1995, 55:4722–4728
32. Calabresi P, Dexter DL, Heppner GH: Clinical and pharmacological implications of cancer cell differentiation and heterogeneity. Biochem Pharmacol 1979, 28:1933–1941
33. Vermeulen SJ, Chen TR, Speleman F, Nollet F, Van Roy FM, Mareel MM: Did the four human cancer cell lines DLD-1. HCT-15, HCT-8, and HRT-18 originate from one and the same patient? Cancer Genet Cytogenet 1998, 107:76–79
34. Rodrigues NR, Rowan A, Smith ME, Kerr IB, Bodmer WF, Gannon JV, Lane DP: p53 mutations in colorectal cancer, Proc Natl Acad Sci USA 1990, 87:7555–7559
35. Vermeulen SJ, Debruyne PR, Marra G, Speleman FP, Boukamp P, Jiricny J, Cuthbert AP, Newbold RF, Nollet FH, van Roy FM, Mareel MM: hMSH6 deficiency and inactivation of the αE-catenin invasion-suppressor gene in HCT-8 colon cancer cells. Clin Exp Metastasis 1999, 17:663–668
36. Morin PJ, Sparks AB, Korinek V, Barker N, Clevers H, Vogelstein B, Kinzler KW: Activation of β-catenin-Tcf signaling in colon cancer by mutations in β-catenin or APC. Science 1997, 275:1787–1790
37. Shirasawa S, Furuse M, Yokoyama N, Sasazuki T: Altered growth of human colon cancer cell lines disrupted at activated Ki-ras. Science 1993, 260:85–88
38. Shahrzad S, Quayle L, Stone C, Plumb C, Shirasawa S, Rak JW, Coomber BL: Ischemia-induced K-ras mutations in human colorectal cancer cells: role of microenvironmental regulation of MSH2 expression. Cancer Res 2005, 65:8134–8141
39. Shahrzad S, Shirasawa S, Sasazuki T, Rak JW, Coomber BL: Low-dose metronomic cyclophosphamide treatment mediates ischemia-dependent K-ras mutation in colorectal carcinoma xenografts. Oncogene 2008, 27:3729–3738
40. Roe S, Koslov ER, Rimm DL: A mutation in α-catenin disrupts adhesion in clone A cells without perturbing its actin and β-catenin binding activity. Cell Adhes Commun 1998, 5:283–296
41. Zheng PS, Wen J, Ang LC, Sheng W, Viloria-Petit A, Wang Y, Wu Y, Kerbel RS, Yang BB: Versican/PG-M G3 domain promotes tumor growth and angiogenesis. FASEB J 2004, 18:754–756
42. Hamid R, Rotshteyn Y, Rabadi L, Parikh R, Bullock P: Comparison of alamar blue and MTT assays for high through-put screening. Toxicol In Vitro 2004, 18:703–10
43. Nakayama GR, Caton MC, Nova MP, Parandoosh Z: Assessment of the Alamar Blue assay for cellular growth and viability in vitro. J Immunol 1997, 204:205–8
44. Papaioannou VE, Fox JG: Efficacy of tribromoethanol anesthesia in mice. Lab Anim Sci 1993, 43:189–192
45. Fathers KE, Stone CM, Minhas K, Marriott JJ, Greenwood JD, Dumont DJ, Coomber BL: Heterogeneity of Tie2 expression in tumor microcirculation: influence of cancer type, implantation site, and response to therapy. Am J Pathol 2005, 167:1753–1762
46. Yu JL, Rak JW, Carmeliet P, Nagy A, Kerbel RS, Coomber BL: Heterogeneous vascular dependence of tumor cell populations. Am J Pathol 2001, 158:1325–1334
47. Yu JL, May L, Lhotak V, Shahrzad S, Shirasawa S, Weitz JI, Coomber BL, Mackman N, Rak JW: Oncogenic events regulate tissue factor expression in colorectal cancer cells: implications for tumor progression and angiogenesis. Blood 2005, 105:1734–1741
48. Tucker RW, Sanford KK, Handleman SL, Jones GM: Colony morphology and growth in agarose as tests for spontaneous neoplastic transformation in vitro. Cancer Res 1977, 37:1571–1579
49. Chaplin DJ, Durand RE, Olive PL: Cell selection from a murine tumour using the fluorescent probe Hoechst 33342. Br J Cancer 1985, 51:569–572
50. Rosenthal KL, Tompkins WA, Frank GL, McCulloch P, Rawls WE: Variants of a human colon adenocarcinoma cell line which differ in morphology and carcinoembryonic antigen production. Cancer Res 1977, 37:4024–4030
51. Tompkins WA, Watrach AM, Schmale JD, Schultz RM, Harris JA: Cultural and antigenic properties of newly established cell strains derived from adenocarcinomas of the human colon and rectum. J Natl Cancer Inst 1974, 52:1101–1110
52. Agazie YM, Hayman MJ: Molecular mechanism for a role of SHP2 in epidermal growth factor receptor signaling. Mol Cell Biol 2003, 23:7875–7886
53. Vécsey-Semjén B, Becker KF, Sinski A, Blennow E, Vietor I, Zatloukal K, Beug H, Wagner E, Huber LA: Novel colon cancer cell lines leading to better understanding of the diversity of respective primary cancers. Oncogene 2002, 21:4646–4662
54. Debruyne PR, Vermeulen SJ, Berx G, Pocard M, Correia da Rocha AS, Li X, Cirnes L, Poupon MF, van Roy FM, Mareel MM: Functional and molecular characterization of the epithelioid to round transition in human colorectal cancer LoVo cells. Oncogene 2003, 22:7199–7208
55. Woerner SM, Kloor M, von Knebel Doeberitz M, Gebert JF: Microsatellite instability in the development of DNA mismatch repair deficient tumors. Cancer Biomark 2006, 2:69–86
56. Schwartz S Jr, Yamamoto H, Navarro M, Maestro M, Reventos J, Perucho M: Frameshift mutations at mononucleotide repeats in caspase-5 and other target genes in endometrial and gastrointestinal cancer of the microsatellite mutator phenotype. Cancer Res 1999, 59:2995–3002
57. da Costa LT, Liu B, el-Deiry W, Hamilton SR, Kinzler KW, Vogelstein B, Markowitz S, Willson JK, de la Chapelle A, Downey KM, So AC: Polymerase δ variants in RER colorectal tumours. Nat Genet 1995, 9:10–11
58. Li HR, Shagisultanova EI, Yamashita K, Piao Z, Perucho M, Malkhosyan SR: Hypersensitivity of tumor cell lines with microsatellite instability to DNA double strand break producing chemotherapeutic agent bleomycin. Cancer Res 2004, 64:4760–4767

59. Lamlum H, Papadopoulou A, Ilyas M, Rowan A, Gillet C, Hanby A, Talbot I, Bodmer W, Tomlinson I: APC mutations are sufficient for the growth of early colorectal adenomas, Proc Natl Acad Sci USA 2000, 97:2225–2228
60. Vermeulen SJ, Nollet F, Teugels E, Vennekens KM, Malfait F, Philippe J, Speleman F, Bracke ME, van Roy FM, Mareel MM: The αE-catenin gene (CTNNA1) acts as an invasion-suppressor gene in human colon cancer cells. Oncogene 1999, 18:905–915
61. Morton RA, Ewing CM, Nagafuchi A, Tsukita S, Isaacs WB: Reduction of E-cadherin levels and deletion of the α-catenin gene in human prostate cancer cells. Cancer Res 1993, 53:3585–3590
62. Oda T, Kanai Y, Shimoyama Y, Nagafuchi A, Tsukita S, Hirohashi S: Cloning of the human α-catenin cDNA and its aberrant mRNA in a human cancer cell line. Biochem Biophys Res Commun 1993, 193:897–904
63. Vanpoucke G, Nollet F, Tejpar S, Cassiman JJ, van Roy F: The human αE-catenin gene CTNNA1: mutational analysis and rare occurrence of a truncated splice variant. Biochim Biophys Acta 2002, 1574:262–268